INTER-NOISE 2007

28-31 AUGUST 2007
ISTANBUL, TURKEY

Numerical noise prediction: application to radial fans

Yilmaz Dogan[a], Esra Sorguven[b], Faruk Bayraktar[c], Kenan Y. Sanliturk[d]

Arçelik A.Ş.R & D Department
Vibration & Acoustic Technologies
Tuzla, 34950 Istanbul
TURKEY

ABSTRACT

In this study, aerodynamics and aeroacoustics of two radial fans are investigated by using a hybrid computational aeroacoustics method. Unsteady turbulent flow field of both fans is simulated with large eddy simulation (LES). Acoustic sources are computed based on the pressure fluctuations. Inhomogeneous wave equation, which accounts for the propagation, diffraction and scattering of the acoustic sources inside the volute, is solved to determine the far field sound pressure level with the boundary element method. Numerically obtained sound pressure level distributions are in a good agreement with experimental data. Sound pressure level distribution in narrow band frequency spectrum, directivity of the acoustic waves and the overall sound power level are predicted numerically with a high accuracy. Furthermore, results of the LES provide an insight to the turbulent flow and noise generation mechanisms.

1 INTRODUCTION

Flow induced noise prediction in industrial applications is essential in order to control the noise emission and to comply with the noise regulations and consumer demands. Experimental methods involve drawbacks like time and investment expenses and measurement errors like reflection problems. With the improvement in computational technology, aomputational aeroacoustics (CAA) provides a proper model for noise prediction and reduction. Especially hybrid CAA methods are efficient and inexpensive, since they solve for the different scales of aerodynamics and aeroacoustics separately.

Studies on aeroacoustics began after the 2nd World War, as the civil aircraft technology has evolved. In his acoustic analogy, Lighthill [1, 2] derived an inhomogeneous wave equation to describe the jet noise, which arises due to turbulent pressure fluctuations, for describing the radiation of the sound field generated by turbulent flow. Curle [3] contributed the effect of solid surfaces on sound generation and by Ffowcs Williams and Hawkings [4] the effect of moving solid surfaces on sound generation is contributed to the acoustic analogy. Numerical methods for the prediction of fan noise usually account for tonal and broadband noise separately. Gutin[5], Carolus [6] and Bommes et. al. [7] have made notable contributions to the aerodynamics and the acoustics of the fans. A recent review on computational aeroacoustics has been provided by Colonius and Lele [8].

[a] Email address: yilmaz.dogan@arcelik.com
[b] Email address: sorguven@yeditepe.edu.tr
C Email address: faruk.bayraktar@arcelik.com
C Email address: sanliturk@itu.edu.tr

Studies involving analysis, prediction and reduction of fan noise are active research areas because of the widespread use of axial and centrifugal fans in industry. Lin et. al. [9] designed a small Forward–Curved (FC) centrifugal fan under the space limitations of notebook computers with the emphasis on the blade shape, blade inlet angle and the outlet geometry of the housing and the flow patterns throughout the fan are visualized using numerical techniques. Jeon et. al. [10] developed a method to calculate the unsteady flow fields and Aeroacoustic sound pressure in the centrifugal fan of a vacuum cleaner: Unsteady flow-field data are calculated by the vortex method. The sound pressure is then calculated by an acoustic analogy. Nallasamy et. al. [11] studied the rotor wake turbulence stator interaction broadband noise. The computations employ the wake flow turbulence information from computational fluid dynamic solutions. Gérard et. al. [12] developed an inverse Aeroacoustic model aiming at reconstructing the aerodynamic forces (dipole strength distribution) acting by the fan blades at multiples of the Blade Passing Frequency (BPF) on the fluid that relates the unsteady forces to the radiated sound field. Velarde et. al. [13] studied the experimental determination of the tonal noise sources in a centrifugal fan. Özyörük et. al. [14] developed a frequency-domain method for predicting sound fields of ducted fans based on the solution of the frequency-domain form of the Euler equations linearized about an axisymmetric non-uniform background flow. Wu et. al. [15] developed a semi-empirical formula capable of simulating both narrow and broad band sounds of the spectra for the tested axial flow fans in a free-field. Wu et. al. [16] also developed a computer model for estimating the noise performance of an engine cooling fan assembly. The computer model thus obtained is validated experimentally on five sets of completely different engine cooling fan assemblies. Velarde et. al. [17] studied a three-dimensional numerical simulation of the complete unsteady flow on the whole impeller-volute configuration of a centrifugal fan. It is claimed that, numerical results have been confirmed using experimental investigations, showing a good agreement.

In this paper, aerodynamics and aeroacoustics of two radial fans are investigated via CAA. For this purpose a hybrid method is employed. Aeroacoustic computations of both fans are performed in two steps: i) computing the unsteady flow field and ii) computing the acoustic pressure fluctuations in the far field in the frequency domain. Flow field is solved with Large Eddy Simulation (LES) where the large and energetic scales of turbulence are resolved and the small and dissipative scales are modeled. Acoustic sources are computed based on the turbulent unsteady flow field. Finally, the wave equation is solved to determine the far field sound pressure level. It is shown that the numerical results of the turbulent unsteady flow and noise emission are in good agreement with the experimental results. Computing the aerodynamics and aeroacoustics data of both fans also shows how the CAA methods provide an insight to the turbulent flow and the noise generation mechanisms and how these can be utilized to decrease the overall sound pressure level of a fan.

2 COMPUTATIONAL METHODS

2.1 Computational Fluid Dynamics

An overview of the modern CAA methods is given in Fig.1. As can be seen in this figure, modern CAA techniques can be separated into two steps; the first step being the determination of the unsteady flow data (flow calculation) and the second step being the computation of the acoustic data (acoustic calculation). Flow calculation can be performed with unsteady Reynolds Averaged Navier-Stokes equations (uRANS), Large Eddy Simulation (LES) or Direct Numerical Simulation (DNS). Flow parameters can be divided as follows: $\overline{\phi}$ is the mean value, $\phi_{turb.}$ is the turbulent part and $\phi_{ac.}$ is the acoustic part of the flow parameters. Although uRANS requires relatively low computational time and power, it cannot handle the unsteady flow accurately. However DNS aims to solve the Navier-Stokes equation without any modeling approximations and aims to resolve the whole range of time and length scales; from integral scales to Kolmogorov scales. With DNS, one can solve all the scales and obtain the mean, turbulent and acoustic parts of the flow parameters. The main disadvantage of such methods is the enormous computational cost of such direct calculations, this being the main reason for which only relatively simple flow configurations at modest Reynolds numbers were studied.

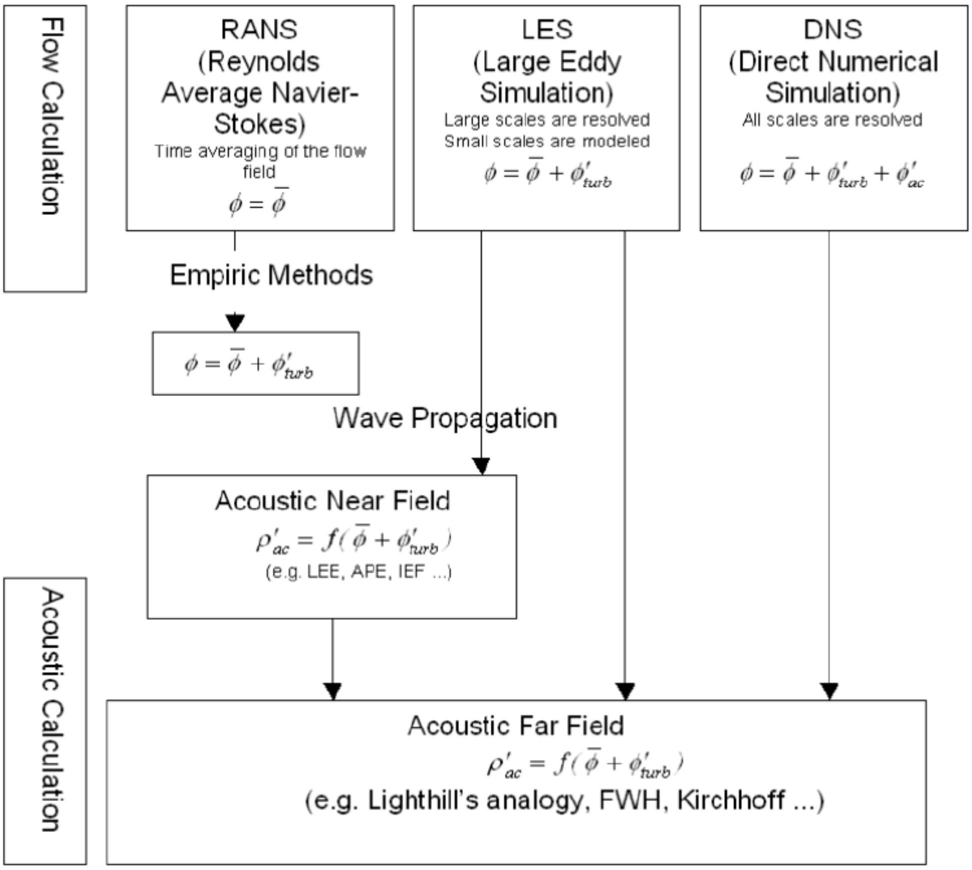

Figure1: Overview of the modern CAA methods

In this paper LES method, which resolves the large and energetic scales of turbulence and models the small and dissipative scales, is used to calculate the unsteady flow field.

2.2 Investigated fans

Two radial fan systems with their volute and inlet and outlet pipes are investigated. The first radial fan system- called"Fan I" has a higher sound pressure levels than the radial fan system called "Fan II".

Both of the investigated radial fan systems are nearly 50 cm long and have a rotational speed of 2800 rpm (Fig. 2). The impeller of Fan I with 37 forward curved blades has an outer diameter of 130 mm and a depth of 55 mm. Accordingly, Reynolds number based on the blade tip diameter and speed is Re_{tip} =136,000 and Mach number at the tip is M_{tip} =0.05. The impeller of Fan II with 25 forward curved blades, has an outer diameter of 120 mm and a depth of 85 mm. Accordingly, Reynolds number based on the blade tip diameter and speed is Re_{tip} =110,000 and Mach number at the tip is M_{tip} =0.05.

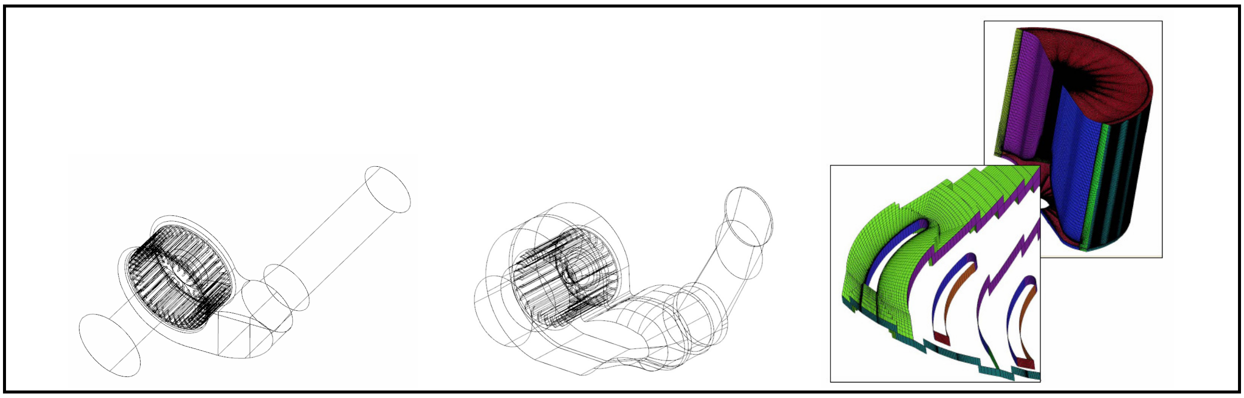

Figure2: Geometry of the investigated fans (left: Fan I, right: Fan II) and the computational mesh

Computational mesh for individual fans comprises approximately 2.5x10^{6} control volumes (Fig. 2). Although the total number of control volumes seems to be insufficient for an LES, the density of the control volumes is increased in the vicinity of the fan blades, where most of the sound emission occurs. Cell distribution is forced to be finer on the walls to resolve the boundary layer and in the neighborhood of the blade. The dimensionless wall distance y+ is kept about 1 over the whole propeller surface and the use of a wall model is omitted. Mesh elements surrounding the impeller are structured and hexahedral, whereas tetrahedral elements are used in the volute.

The computational domain is divided into two zones, one surrounding the rotating impeller and other surrounding the stationary volute. Zones are coupled via a sliding interface and mass balance is forced across the sling interface. In order to minimize the interpolation errors, the ratio of the control volumes across the sliding interface is kept below 4:1. The employed boundary conditions are no-slip at the walls, constant total pressure at the inlet and constant static pressure at the outlet. The computational domain is initialized with the flow data obtained from a steady RANS simulation, in order to accelerate convergence. Spatial discretization is performed with the 2nd order central differencing scheme and temporal discretization with the 2nd order implicit dual time stepping scheme. The aerodynamical and acoustic time steps are set equal as 1x10^{-4} s, i.e. about 1° of rotation of fan is simulated at each time step.

Pressure fluctuations on the surfaces are recorded after nearly five rotations of the fans, so that only statistically steady data are evaluated in the acoustic computation. After the statistically steady state is achieved, flow simulations are continued further for about 5 revolutions of the Fan I, i.e. for 0.107 seconds and about 3 revolutions of the Fan II, i.e. for 0.064 seconds. The dipoles are computed depending on the flow data of these last revolutions. Among the three types of sound sources (i.e. monopoles, dipoles and quadrupoles) the dipole terms dominate the sound emission in a turbomachinery [18].

2.3 Acoustic Computation

The aeroacoustic modeling is performed with the aeroacoustic module of the vibroacoustic solver LMS Sysnoise. Sysnoise is capable of solving wave equation in interior and exterior domains with different discretization techniques like Boundary Element Method (BEM) and Finite Element Method (FEM) [19].

The input for aeroacoustic module is time-dependent pressure and velocity data which are obtained from the CFD solution. The flow data are used to calculate the acoustic source terms on the right hand side of the wave equation.

In order to model the interior and the exterior domains simultaneously, the Multi-Domain BEM analysis is performed. The analysis consists of two models which are the Direct BEM Interior and the Direct BEM Exterior models. Both models are linked at the openings of the duct, through a fluid-fluid coupling. The coupling satisfies the boundary condition at the openings, equivalent to ambient pressure boundary condition. The boundary condition applied on the duct surface is the rigid wall boundary condition. The stationary dipole sources on the duct surface are defined as discrete sound sources on the nodes of the acoustic mesh.

3 RESULTS

3.1 Computational Fluid Dynamic

The following figures aim to give an overview of the flow around the fan and inside the volute.

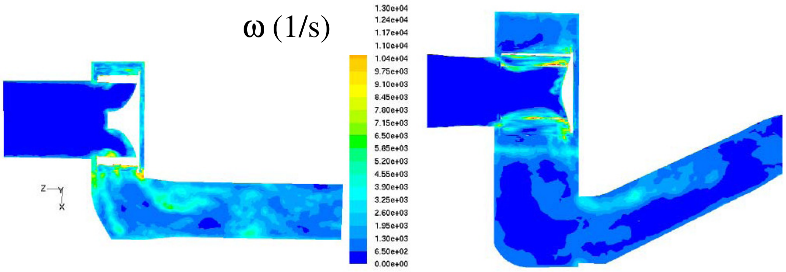

Figure 3: Instantaneous picture of the magnitude of the vorticity (left: Fan I, right: Fan II)

Figure 3 shows the instantaneous magnitude of the vorticity at a cross-section along the flow domain. The vorticity is produced mainly on the blades; especially at the blade tip and on the trailing edge. It is then transported further with the flow through the pipe. From figures it can be seen that although the vorticity produced is similar in both fan impellers, in Fan I the vorticity is transported further into the outlet pipe.

3.2 Computational Aero Acoustics

Computational grid for Aeroacoustic calculations is created using the 3D drawing/FEM solver in I-DEAS. Aeroacoustic computational grid is coarse; hence, an external MATLAB interface code is used for interpolation between fine CFD mesh and coarse Aeroacoustic mesh.

Aeroacoustic computation involves two steps:

i) Assigning the dipole sources over the Aeroacoustic mesh

ii) Coupling between the Multi Domain Boundary Element Method (MDBEM) – Interior and MDBEM – exterior to model the acoustic modes of the cavity.

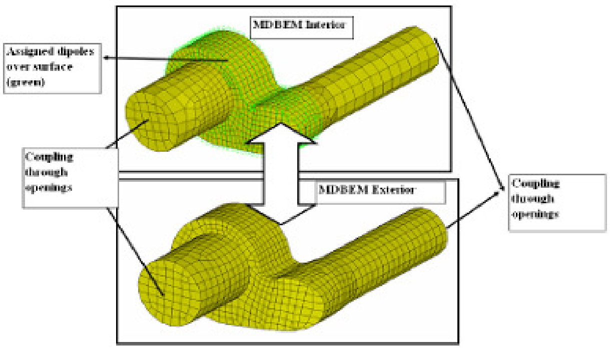

Figure 5: Coupling procedure for fans

In Fig. 5, MDBEM Exterior and MDBEM Interior models are shown for Fan I. With assigned dipoles on Interior model, both models are coupled via openings to calculate the cavity modes of the volute and also scattering phenomenon.

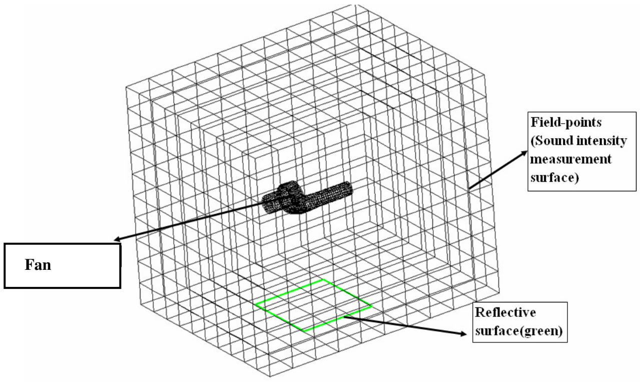

Figure 6: I-BEM model and sound radiation model for current design

In Fig. 6, a fictitious surface used in both experiments and numerical calculations is shown. The physical and numerical systems have a reflective surface and field points to measure sound intensity.

Numerical results of the two radial fans are summarized in Fig. 8. The acoustical results are obtained according to sound intensity mapping. A field point mesh is created for both fans, which corresponds the microphone positions of the experiments.

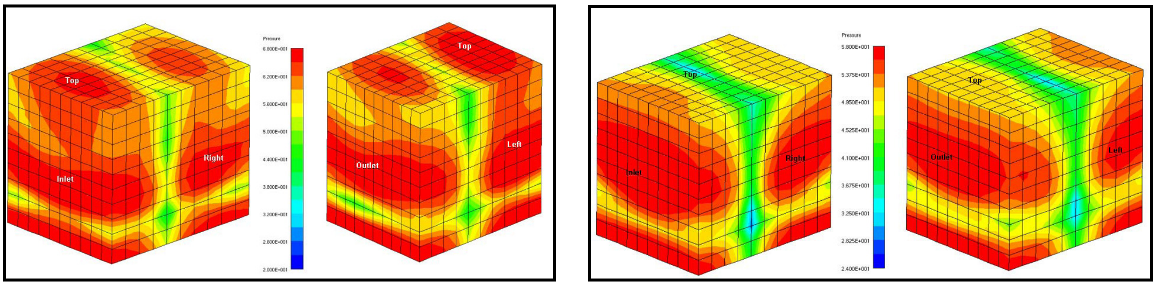

Figure 8: Numeric sound intensity mapping over the field point (left: Fan I, right: Fan II (1/12 octave band))

Fan II has a lower sound power level with respect to that of Fan I (Fig. 8). With the same color scale range, the directivity shows different characteristics from one cavity frequency to another. However, the magnitude of the sound pressure levels is different, but directivity patterns are very similar for the two different fans.

4 MEASUREMENTS AND COMPARISION WITH NUMERICAL RESULTS

Sound intensity measurements are performed for the two fans over a rectangular box in which fans are located. Sound intensity is the time-averaged product of the pressure and particle velocity. Therefore, it is possible to measure pressure gradient with two closely spaced microphones and relate it to particle velocity.

The use of sound intensity rather than sound pressure to determine the sound power allows to perform the measurement in situ. The sound power is the average normal intensity over a surface enclosing the source, in this case fan-volute system, multipled by the surface area. The fictitious surface and the reflective floor are the same as in the numerical computation (Fig. 6).

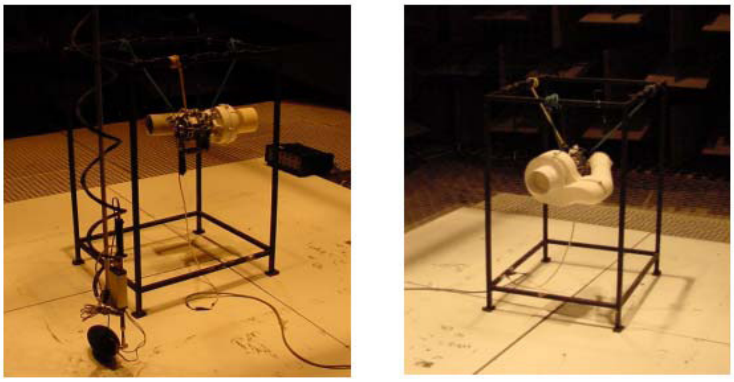

Figure 9: Experimental set-up for both sound intensity and sound pressure measurements (left: Fan I, right: Fan II)

The experimental Sound Pressure Level (SPL) curve is smoother than the numerical curve. The reason for this is related to the amount of data used to obtain these results: In the experiments, the acoustic signal is measured for about 10 s. However, in the simulation the total time for the acoustic evaluation is about 0.107 s for Fan I and 0.064 s for Fan II which corresponds to about 5 and 3 rotations of the propeller. In the experiments the acoustic signal of about 500 rotations is evaluated. Since the frequency analysis is performed with far less data in the simulation than what is available in the experiment. Therefore, the numerical SPL curve has more fluctuations than the experimental curve. If the acoustic computation is carried out for longer time, these fluctuations will disappear, but the general shape of the curve will remain the same.

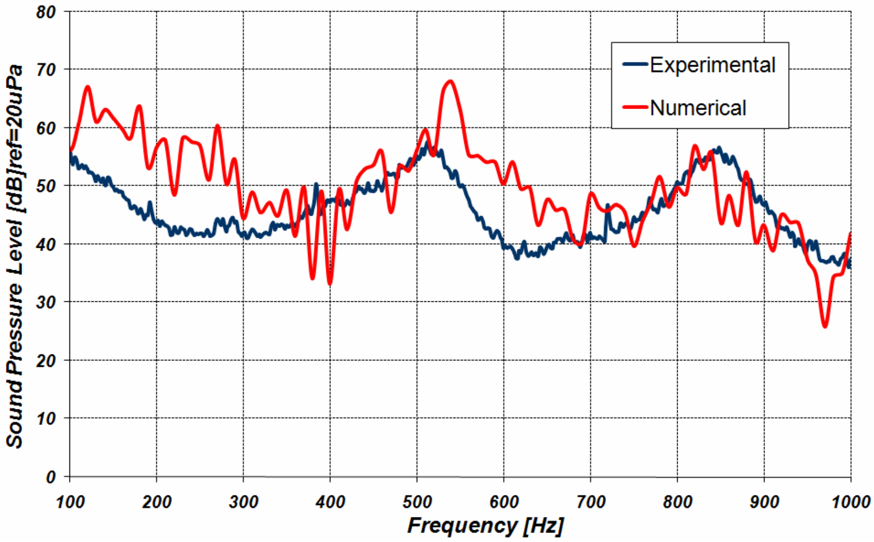

Figure 10: Sound pressure level spectrum from computations and experiments of Fan I

As can be seen in Fig.10, the numerical prediction of the acoustic signal in the far field matched the experimental measurements satisfactorily for Fan I.

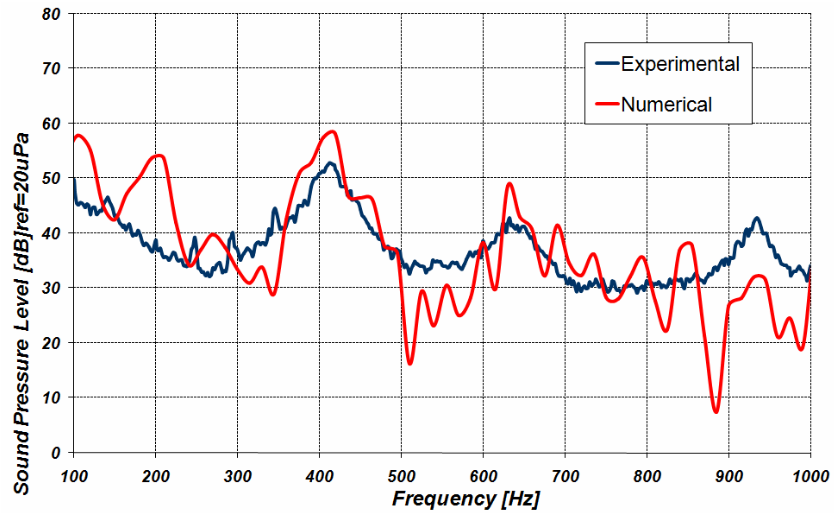

Figure 11: Sound pressure level spectrum from computations and experiments of Fan II

As seen in Fig.11 that the acoustic prediction agrees well with the experimental measurements in the case of Fan II.

From Figures 12-13, one can see that for both fans, the CAA-tool is tested with high accuracy. The first test case is the prediction of the flow noise of a radial fan currently used in laundry dryers with high SPL. Simulations of the flow in the flow domain of fan-volute system show that LES is a reliable flow simulation method. The aerodynamical characteristics of the flow are predicted with high accuracy. Consequently, the acoustic prediction and directivity of the sound agrees well with the experimental measurements.

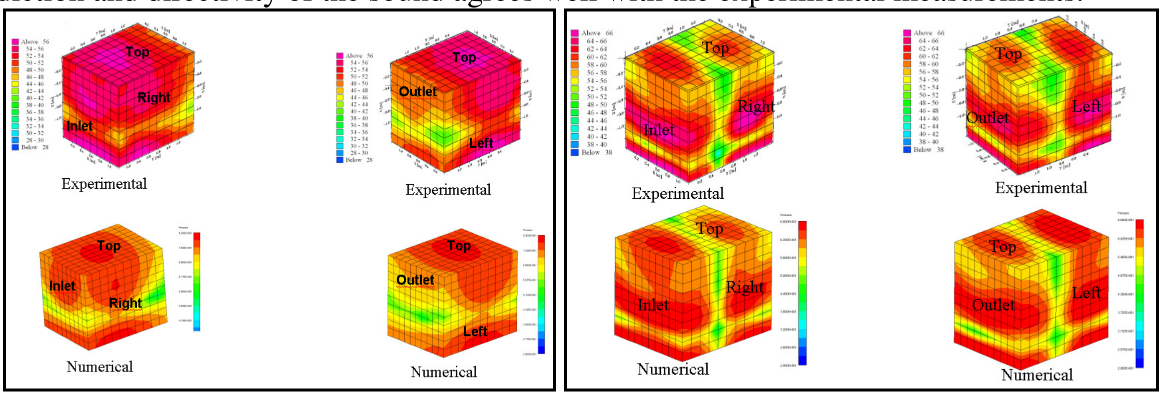

Figure 12: Numerical and experimental sound intensity mapping over the field point for Fan I (270Hz and 520 Hz respectively (1/12 octave band))

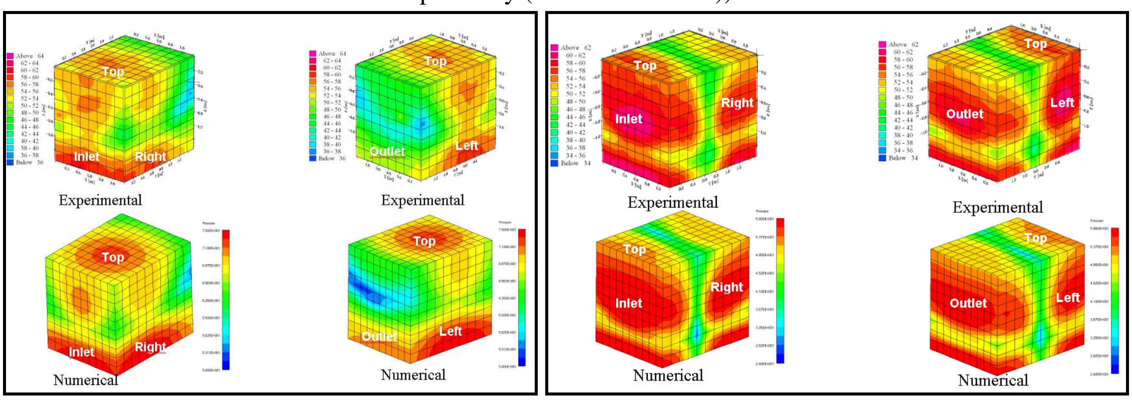

Figure 13: Numerical and experimental sound intensity mapping over the field point for Fan II (240 Hz and 420 respectively (1/12 octave band))

5 CONCLUDING REMARKS

In the frame of this work, far field noise of two radial fans is predicted numerically. The first test case is a radial fan, which is currently used in laundry dryers and has a high sound power level. The second test case is another radial fan-volute system that is designed to replace the first system and has a lower sound power level. This configuration is an enhancement of the first test case. The numerical prediction of the acoustic signal in the far field of both fans matched the experimental measurements satisfactorily.

The presented CAA tool is proven to be a valuable tool for the far field noise prediction. Since the CAA-tool is satisfactorily validated, the tool can be employed in the near future for designing low noise fan systems.

6 REFERENCES

[1] Lighthill, J. M., 1952. On sound generated aerodynamically. I. General theory, Proceedings of the Royal Society of London (A), 211, pp. 564-587.

[2] Lighthill, J. M., 1954. On sound generated aerodynamically. II. Turbulence as a source of sound, Proceedings of the Royal Society of London (A), 222, pp. 1-32.

[3] Curle, N., 1955. The influence of solid boundaries upon aerodynamic sound, Proc. of the Royal Society, Vol. A 231, pp. 505-514.

[4] Ffowcs Williams, J. E., Hawkings, D. L., 1969. Sound generation by turbulence and surfaces in arbitrary motion, Philosophical Transactions of the Royal Society, Vol. A 264, 1151, pp. 321-342.

[5] Gutin, L., 1948. On the sound of a rotating propeller, Zhurnal tekhnicheskoĭ fiziki, 6, 899-909, translated as NACA TM 1195.

[6] Carolus, T., 2003, Ventilatoren – Aerodynamischer Entwurf, Schallvorhersage, Konstruktion, Teubner Verlag, Wiesbaden

[7] Bommes, L., Fricke, J., Klaes, K., 2003, Ventilatoren, Vulkan Verlag, Essen,.

[8] Colonius, T., Lele, S. K., 2004. Computational aeroacoustics: progress on nonlinear problems of sound generation. Progress in Aerospace Sciences 40, 345-416.

[9] Lin, S.C., Huang, C.L., 2001, An integrated experimental and numerical study of forward-curved centrifugal fan , Experimental Thermal and Fluid Science 26, pp. 421-434,.

[10] Jeon, W.H., Baek, S.J., Kim, C.J., 2002, Analysis of the aeroacoustic characteristics of the centrifugal fan in a vacuum cleaner, Journal of Sound and Vibration 268, pp. 1025-1035,.

[11] Nallasamy, M., Envia, E., 2005, Computation of rotor wake turbulence noise, Journal of Sound and Vibration 282, pp. 649-678,.

[12] Gerard, A., Berry, A., 2005, Control of tonal noise from subsonic axial fan. Part 1: reconstruction of aeroacoustic sources from far-field sound pressure, Journal of Sound and Vibration 288, pp. 1049-1075,.

[13] Velarde, S., Tajadura, R., 2006, Experimental determination of the tonal noise sources in a centirfugal fan, Journal of Sound and Vibration 295, pp. 781-796,.

[14] Özyörük, Y., Alpman, E., 2004, Frequency-domain prediction of turbofan noise radiation, Journal of Sound and Vibration 270, pp. 933-950,.

[15] Wu, S.F., Su, S., 1997, Modeling of the noise spectra of axial flow fans in a free field, Journal of Sound and Vibration 200, pp. 379-399,.

[16] Wu, S.F., Su, S., 1998, Noise radiation from engine cooling fans, Journal of Sound and Vibration 216, pp. 107-132,.

[17] Velarde, S., Tajadura, R., 2006, Numerical simulation of the aerodynamic tonal noise generation in a backward-curved blades centrifugal fan, Journal of Sound and Vibration 295, pp. 781-796,.

[18] Goldstein, M. E., 1976. Aeroacoustics, McGraw-Hill Book Company, New York.

[19] Page, G. J., McGuirk, J. J., Hossain, M., Self, R., Bassetti, A., 2003, A CFD coupled acoustic approach for coaxial jet noise, AIAA paper, AIAA 2003-3286,.